

Accepted Manuscript

Photophysical properties of Schiff's bases from 3-(1,3-benzothiazol-2-yl)-2-hydroxy naphthalene-1-carbaldehyde

Manjaree A. Satam, Rahul D. Telore, Nagaiyan Sekar

PII: S1386-1425(14)00808-7
DOI: <http://dx.doi.org/10.1016/j.saa.2014.05.029>
Reference: SAA 12191

To appear in: *Spectrochimica Acta Part A: Molecular and Biomolecular Spectroscopy*

Received Date: 9 February 2014
Revised Date: 1 May 2014
Accepted Date: 12 May 2014

Please cite this article as: M.A. Satam, R.D. Telore, N. Sekar, Photophysical properties of Schiff's bases from 3-(1,3-benzothiazol-2-yl)-2-hydroxy naphthalene-1-carbaldehyde, *Spectrochimica Acta Part A: Molecular and Biomolecular Spectroscopy* (2014), doi: <http://dx.doi.org/10.1016/j.saa.2014.05.029>

This is a PDF file of an unedited manuscript that has been accepted for publication. As a service to our customers we are providing this early version of the manuscript. The manuscript will undergo copyediting, typesetting, and review of the resulting proof before it is published in its final form. Please note that during the production process errors may be discovered which could affect the content, and all legal disclaimers that apply to the journal pertain.



**Photophysical properties of Schiff's bases from 3-(1,3-benzothiazol-2-yl)-2-hydroxy
naphthalene-1-carbaldehyde**

Manjaree A. Satam, Rahul D. Telore, Nagaiyan Sekar*

Tinctorial Chemistry Group, Department of Dyestuff Technology, Institute of Chemical
Technology, Matunga, Mumbai-400 019, India.

E-mail: n.sekar@ictmumbai.edu.in, nethi.sekar@gmail.com

Tel: +91 22 3361 2707; Fax: +91 22 3361 1020.

Abstract:

A series of novel Schiff's bases have been synthesized from 3-(1,3-benzothiazol-2-yl)-2-hydroxynaphthalene-1-carbaldehyde. The presence of hydroxyl group ortho to the benzothiazolyl group as well as the imine linkage lead to the occurrence of excited state intramolecular proton transfer process. The computational strategy was used to study the ESIPT process of the synthesized Schiff's bases, which revealed surprisingly that the keto form predominantly exists in the ground state contradicting the ESIPT process. Density functional theory and time dependent density functional theory have been used to investigate the structural parameters and photophysical properties in different solvents of one of the Schiff's bases. The experimental results correlate well with the computed results. All Schiff's bases show good thermal stability.

Keywords: Schiff's base, benzothiazole, imine linkage, photophysical property, ESIPT, density functional theory.

1. Introduction:

The reaction between amine and aldehyde functions resulting in the formation of Schiff's bases having conjugated carbon-nitrogen double bonds is well known in synthetic organic chemistry [1]. The formation of Schiff's bases has great interest in medicinal chemistry and

material sciences [2] as they form very stable complexes with the metal ions [3-7]. Mostly the Schiff's bases are used as metal sensors [7-10] as well as optical pH sensor [11].

The metal-ion sensing is carried out using fluorescence spectroscopy because of high sensitivity, low cost and instant response [12-16]. The ratiometric fluorescence sensors have been used over the conventional method for fluorescence based sensing applications [17-20]. The ratiometric fluorescence sensors with excited state intra molecular proton transfer (ESIPT) have a great importance as they provide dual emitting channel [21, 22]. Singh N. *et al.* have synthesized substituted 1-((phenylimino)methyl)naphthalene-2-ol as a metal-ion sensor undergoing ESIPT process for the detection of Mg^{2+} ion [23]. Udhayakumari D. *et al.* have synthesized simple imine linked salicylaldimine based Schiff's base for the detection of Zn^{2+} ion. On binding with the metal-ion, this sensor shows a fluorescence enhancement due to the inhibition of the ESIPT mechanism [24].

In the last decade study of ESIPT has gained considerable attention in terms of the experimental as well as the theoretical studies [25, 26]. The molecules exhibiting ESIPT are often used to develop new functional molecules such as laser dyes [27, 28], fluorescent probes in biology [29] and light-emitting materials for electroluminescent devices [30], higher energy radiation detectors, polymer protectors [31-32]. The molecules with ESIPT character often show large Stokes shift [33-35]. Stabilisation of different tautomers of ESIPT molecules are highly influence by solvent polarity [36, 37]. Guha *et al.* investigated the proton transfer reaction occurring in 7-ethylsalicylidenebenzylamine and have concluded that this molecule exists in more than one structural form in most of the protic solvents [37]. The fluorescence intensity is influenced by the microenvironment, like viscosity of the solvent, temperature and pH [38-42]. The photophysical properties of Schiff's base containing an intramolecular hydrogen bond have

also been studied by using steady state and time resolved fluorescence spectroscopy [38, 39]. Recently quantum chemical computational studies have been used in structural optimization, and in understanding the photophysical properties, and nonlinear optical properties of salen type Schiff's base [43].

In continuation of our previous work [44], the current study describes the synthesis and photophysical properties of novel Schiff's bases, and the effect of the solvent polarity on the photophysical properties of Schiff's bases **6a-6f** (**Scheme 1**). Also the structure optimization of one of the synthesized Schiff's base **6a** was carried out both in the ground and the excited state by using density functional theory (DFT) to study ESIPT process but anomalous results were obtained. DFT study reveals that the keto form predominantly exists in the ground state and not the enol form. Thus there is no existence of ESIPT process in these synthesized Schiff's bases. Experimental results also support this as these molecules observed small Stokes shift unlike the ESIPT molecules.

2. Experimental section:

2.1. Materials and equipments:

All the reagents and solvents were purchased from Sd Fine Chemicals Pvt. Ltd and used without purification. All solvents used were of spectroscopic grade. Melting point was recorded by open capillary on Sunder Industrial Product and is uncorrected. The reactions were monitored using pre-coated silica gel aluminum backed TLC plates; Kiesel gel 60 F₂₅₄ Merck (Germany). The UV-Visible absorption measurements were carried out using a Spectronic Genesys 2 spectrophotometer with 1 cm length quartz cells. The excitation wavelength was taken as λ_{max} of compound. The scan range was 250 to 650 nm. The fluorescence emission measurements were

recorded on Cary Eclipse fluorescence spectrophotometer (Varian, Australia) using 1 cm length quartz cells. The quantum yields of these compounds were calculated using fluorescein ($\Phi_f = 0.91$ in ethanol) [45] as the standard. For this purpose, the absorption and the emission intensities of the Schiff's bases **6a-6f** in all the solvents were recorded at constant interval of concentrations (0.5, 1, 1.5, 2, 2.5 ppm). Also absorption and emission intensities of fluorescein were measured in ethanol (as the quantum yield of fluorescein is reported in ethanol). All the measurements were recorded at constant parameters such as source of light, slit width, cuvette. The absorption intensities were plotted against emission intensities for all solvents. From these graphs, slopes were calculated for each Schiff's bases and the standard. Using these slopes and **Formula 1**, the relative quantum yield of Schiff's bases in different solvents were calculated. The refractive indices of the solvents have been taken from literature [46].

Formula 1 Relative quantum yield

$$\Phi_X = \Phi_{ST} \left(\frac{m_X}{m_{ST}} \right) \left(\frac{\eta_X^2}{\eta_{ST}^2} \right)$$

Where, Φ_X = Quantum yield of analyte

Φ_{ST} = Quantum yield of standard

m_X = slope for analyte

m_{ST} = slope for standard

η_{ST}^2 = Refractive index of solvent for standard

η_X^2 = Refractive index of solvent for analyte

The FT-IR analysis was performed on a FTIR-8400S SHIMADZU spectrophotometer. The thermo gravimetric analyses were carried out on a SDT Q600 TA Instruments. Method for thermo gravimetric analysis was done with ramp 10°C per minute from ambient temperature to

600°C under nitrogen atmosphere. ^1H NMR spectra were recorded on VXR 400-MHz instrument using TMS as an internal standard and DMSO as the solvent. Purification of all the compounds was generally achieved by recrystallization. The purity of compounds was ascertained by thin layer chromatography. The analyses data of all Schiff's bases are given in the supporting information.

2.2. Computational Methods:

The ground state (S_0) geometry of the conformers and tautomers of the Schiff's base **6a** in their C_1 symmetry were optimized using the tight criteria in the gas phase as well as in the different solvents using Density Functional Theory (DFT) [47]. The vibrational frequencies at the optimized structures were computed using the B3LYP/6-31G(d) method to verify that the optimized structures correspond to local minima on the energy surface [48-50]. The vertical excitation energies at the ground-state equilibrium geometries were calculated with Time Dependent Density Functional Theory (TD-DFT) [51-53]. The low-lying first singlet excited state (S_1) of each conformer was relaxed using the TD-DFT to obtain its minimum energy geometry. The difference between the energies of the optimized geometries at the first singlet excited state and the ground state was used in computing the emissions [54, 55]. The frequency computations were also carried out on the low-lying first excited state of the conformers. All the computations were carried out in vacuum and also in the solvents of different polarities using the Polarizable Continuum Model (PCM) [56, 57]. All electronic structure computations were carried out using the Gaussian 09 program [58].

2.3. Synthesis:

2.3.1. Synthesis of 3-(1,3-benzothiazol-2-yl)-2-hydroxynaphthalene-1-carbaldehyde **4**:

Carbaldehyde **4** was synthesized from 3-(1,3-benzothiazol-2-yl)naphthalen-2-ol [59] as previously reported in ref [44].

2.3.2. *General procedure for preparation of Schiff's bases 6a-6f from 3-(1,3-benzothiazol-2-yl)-2-hydroxynaphthalene-1-carbaldehyde 4:*

3-(1,3-Benzothiazol-2-yl)-2-hydroxynaphthalene-1-carbaldehyde **4** (0.0033 mol), substituted aniline **5a-5f** (0.0033 mol) and ammonium bromide (0.0033 mol) were stirred in ethanol (40 mL) for 4 hours. The solid obtained was filtered, washed thoroughly with water, then with methanol and dried to give the corresponding Schiff's bases **6a-6f**.

2.3.2.1. *1-{(E)-[(2-Aminophenyl)imino]methyl}-3-(1,3-benzothiazol-2-yl)naphthalen-2-ol 6a*

Yield: 62%; **M.p.** 212-216°C.

FT-IR (KBr, cm⁻¹): 1608 (C=O, keto); 1545 (C=N, benzothiazole); 1493 (aromatic ring); 1432 (C=N, imine); 723 (C-S).

¹H-NMR ((CD₃)₂SO, δppm): 15.8 (s, 1H, OH); 9.5 (s, 1H, imine); 9.12 (s, 1H, Ar-H); 8.4 (d, 1H, Ar-H); 8.1 (d, 1H, Ar-H); 8.0 (d, 1H, Ar-H); 7.13 (d, 1H, Ar-H); 7.1 (t, 1H, Ar-H); 7.34 (t, 1H, Ar-H); 7.73 (d, 1H, Ar-H); 7.53 (t, 1H, Ar-H); 7.42 (t, 1H, Ar-H); 7.58 (t, 1H, Ar-H); 7.72 (t, 1H, Ar-H); 6.94 (d, 1H, Ar-H); 5.3 (s, 2H, NH₂).

Mass: *m/z* = 396 (M+1).

2.3.2.2. *3-(1,3-Benzothiazol-2-yl)-1-{(E)-[(2-hydroxyphenyl)imino]methyl} naphthalen-2-ol 6b:*

Yield: 65%; **M.p.** 256-260°C.

FT-IR (KBr, cm⁻¹): 3059 (OH); 1610 (C=O, keto); 1541 (C=N, benzothiazole); 1490 (aromatic ring); 1460 (C=N, imine); 746 (C-S).

¹H-NMR ((CD₃)₂SO, δppm): 15.4 (s, 1H, OH); 10.61 (s, 1H, OH); 9.6 (d, 1H, Ar-H); 9.1 (s, 1H, imine); 8.15 (d, 1H, Ar-H); 8.1 (d, 1H, Ar-H); 8.08 (d, 2H, Ar-H); 8.01 (d, 1H, Ar-H); 7.9 (d, 1H, Ar-H); 7.58 (t, 1H, Ar-H); 7.53 (d, 1H, Ar-H); 7.3 (t, 1H, Ar-H); 7.4 (d, 1H, Ar-H); 7.06 (t, 1H, Ar-H); 6.9 (t, 1H, Ar-H).

Mass: *m/z* = 397 (M+1).

2.3.2.3. *1-[(E)-[(2-Amino-5-nitrophenyl)imino]methyl]-3-(1,3-benzothiazol-2-yl) naphthalen-2-ol 6c:*

Yield: 59%; **M.p.** 246-248°C.

FT-IR (KBr, cm⁻¹): 3324 (OH); 1610 (C=O, keto); 1545 (C=N, benzothiazole); 1501 (aromatic ring); 1340 (NO₂); 722 (C-S).

¹H-NMR ((CD₃)₂SO, δppm): 15.9 (s, 1H, OH); 9.7 (s, 2H, NH₂); 9.1 (s, 1H, Ar-H); 8.4 (s, 1H, Ar-H); 8.1 (d, 1H, Ar-H); 8.04 (m, 4H, Ar-H); 7.5 (m, 4H, Ar-H); 6.9 (d, 1H, Ar-H).

Mass: *m/z* = 441 (M+1).

2.3.2.4. *3-(1,3-Benzothiazol-2-yl)-1-[(E)-[(2-hydroxy-5-methylphenyl)imino]methyl] naphthalen-2-ol 6d:*

Yield: 62%; **M.p.** 262-264°C.

FT-IR (KBr, cm⁻¹): 3057 (-OH); 1610 (C=O, keto); 1541 (C=N, benzothiazole); 1488 (aromatic ring); 727 (C-S).

¹H-NMR ((CD₃)₂SO, δppm): 15.4 (s, 1H, OH); 10.3 (s, 1H, OH); 9.5 (d, 1H, imine); 9.1 (s, 1H, Ar-H); 8.4 (d, 1H, Ar-H); 8.1 (s, 1H, Ar-H); 8.0 (d, 1H, Ar-H); 7.98 (t, 1H, Ar-H); 7.94 (s, 1H,

Ar-H); 7.59 (t, 1H, Ar-H); 7.53 (t, 1H, Ar-H); 7.42 (t, 1H, Ar-H); 7.3 (t, 1H, Ar-H); 6.9 (q, 2H, Ar-H); 2.3 (s, 3H, Ar-CH₃).

Mass: $m/z = 411$ (M+1).

2.3.2.5. 3-(1,3-Benzothiazol-2-yl)-1-*[(E)-[(2-hydroxy-5-nitrophenyl)imino]methyl]* naphthalen-2-ol **6e**:

Yield: 52%; **M.p.** 282-284°C.

FT-IR (KBr, cm⁻¹): 3010 (OH); 1618 (C=O keto); 1545 (C=N, benzothiazole); 1496 (aromatic ring); 1334 (NO₂); 728 (C-S).

¹H-NMR ((CD₃)₂SO, δppm): 15.4 (s, 1H, OH); 12.5 (s, 1H, OH); 9.7 (d, 1H, Ar-H); 9.1 (s, 1H, Ar-H); 9.0 (s, 1H, imine); 8.58 (s, 1H, Ar-H); 8.1 (d, 1H, Ar-H); 8.0 (q, 2H, Ar-H); 7.9 (d, 1H, Ar-H); 7.6 (d, 1H, Ar-H); 7.5 (t, 1H, Ar-H); 7.43 (t, 1H, Ar-H); 7.36 (t, 1H, Ar-H); 7.19 (d, 1H, Ar-H).

Mass: $m/z = 442$ (M+1).

2.3.2.6. 3-(1,3-Benzothiazol-2-yl)-1-*[(E)-[(2-hydroxy-4-nitrophenyl)imino]methyl]* naphthalen-2-ol **6f**:

Yield: 55%; **M.p.** 226-230°C.

FT-IR (KBr, cm⁻¹): 3024 (OH); 1618 (C=O, keto); 1541 (C=N, benzothiazole); 1490 (aromatic ring); 1369 (NO₂); 739 (C-S).

¹H-NMR ((CD₃)₂SO, δppm): 15.1 (s, 1H, OH); 11.7 (s, 1H, OH); 9.5 (s, 1H, imine); 9.1 (s, 1H, Ar-H); 8.46-8.32 (d, 2H, Ar-H); 8.2-7.8 (m, 4H, Ar-H); 7.9 (s, 1H, Ar-H); 7.7- 7.2 (m, 4H, Ar-H).

Mass: $m/z = 442$ (M+1).

3. Results and discussions:

3-(1,3-Benzothiazol-2-yl)-2-hydroxynaphthalene-1-carbaldehyde **4** was synthesized by the condensation of 2-aminothiophenol with 3-hydroxynaphthalene-2-carboxylic acid followed by Riemer-Teimann reaction. This synthesized carbaldehyde **4** was further reacted with the substituted amines in ethanol in the presence of ammonium bromide to give the corresponding Schiff's bases **6a-6f** (**Figure 1**). Literature survey shows that ammonium bromide was used for cyclization to form bis-azoles [60]. But in this case only Schiff's bases were formed (**Scheme 1**). All these Schiff's bases were purified by recrystallization using methanol and confirmed by FT-IR, Mass and $^1\text{H-NMR}$ analyses.

< **Please insert Scheme 1:** Synthetic scheme of Schiff's bases **6a-6f** from 3-(1,3-benzothiazol-2-yl)-2-hydroxynaphthalene-1-carbaldehyde **4**>

< **Please insert Figure 1:** Structures of the synthesized Schiff's bases **6a-6f**>

These Schiff's bases are containing -OH group adjacent to the benzothiazole ring as well as =N of imine linkage which are supposed to be responsible for ESIPT process. Some ESIPT based Schiff's bases containing salicylaldimine and naphthaldimine (**Figure 2**) have been used for metal-ion sensing, ratiometric sensing as they produce dual channel for the detection [23, 24].

< **Please insert Figure 2:** ESIPT process observed in known molecules>

The aim of this study is to produce a series of Schiff's bases **6a-6f** undergoing ESIPT process. Contrary to the expectation reversed ESIPT was not observed owing to the fact that the keto tautomers are more stable in the ground state as against the fact that the enol tautomer is more stable in the ground state in the known ESIPT molecules [38, 39]. On UV irradiation, these molecules showed single emission with small Stokes shift.

3.1. Effect of solvent polarity on photophysical properties:

To evaluate the effect of solvent polarity on the photophysical properties of the synthesized Schiff's bases **6a-6f**, the absorption and the emission properties of all the compounds were measured in different solvents of differing polarities. These solvents are varying in polarities, refractive indices, dielectric constants and hydrogen bonding capability which provides different environment. Solvents of varying polarities generally effects on the absorption and the emission behavior of the molecules. Analyses were carried out at room temperature with concentration of the solution 10 ppm. The absorption-excitation-emission data of the Schiff's base **6a** are given in **Figure 3** and **Table 1** (Please refer **Figure S1-S5**, **Tables S1-S5** for photophysical data of remaining Schiff's bases **6b-6f**).

The Schiff's bases **6b-6f** showed dual absorption maxima with almost the same intensity except **6a**, which has a single prominent absorption. The dye **6a** showed absorption maxima in the range of 467 to 482 nm in all solvents. It observed a red shift in DMF as compared to the other solvents. The dyes **6b-6e** showed shorter absorption maxima in the range of 467-479 nm and longer absorption maxima in the range of 494-504 nm. The presences of electron withdrawing nitro group as well as the weakly electron realizing methyl group do not bring about any change in the absorption spectra. The absorbance values of the Schiff's bases **6a-6d** were almost similar in all the solvents. In the case of dyes **6e** and **6f**, the absorbance values changed and it was observed to be lower in methanol and acetonitrile.

The fluorescence emission wavelength and quantum yields of the Schiff's bases **6a-6f** in different solvents are presented in the **Table 1** (**Tables S1-S5**). The emission wavelength of the Schiff's bases experienced a red shift in highly polar aprotic solvents DMF and DMSO. The red shift in DMF may be attributed to the stabilization of the excited state in DMF than in the other

solvents. Also it was observed that the quantum yield of all the Schiff's bases varied in different solvents, but independent of the solvent polarity. The Schiff's base **6a** showed the highest quantum yield in ethyl acetate and the lowest value in ethanol. The dyes **6b**, **6c** and **6f** showed a higher quantum yield in DMF while the dyes **6d** and **6e** showed higher quantum yield in chloroform and tetrahydrofuran respectively as compared to the other solvents.

< Please insert **Figure 3**: Effect of solvent polarity on photophysical properties of Schiff's base

6a>

< Please insert **Table 1**: Absorption- excitation- emission data of Schiff's base **6a**>

3.2. Thermal Stability Study:

To study the thermal stability of Schiff's bases **6a-6f**, thermo gravimetric analyses were carried out in the temperature range of 50-600°C under nitrogen atmosphere. The TGA results concluded that the thermal stability of the synthesized Schiff's bases is range in the range of 235-285°C (**Figure 4**). Above this temperature the Schiff's bases show the major loss in weight. Furthermore the order of stability was found to be $6d > 6a > 6e > 6b > 6c > 6f$. Though there is no definite correlation between the structure and thermal stability is found to be slightly more in the case of Schiff's bases obtained from 2,5-disubstituted anilines. The comparisons of the T_d (decomposition temperature) of Schiff's bases **6a-6f** are given in **Table 2**.

< Please insert **Figure 4**: Thermo gravimetric analysis of Schiff's bases **6a-6f**>

< Please insert **Table 2**: Thermo gravimetric analysis of Schiff's bases **6a-6f**>

3.3. Density functional theory (DFT) Computations

The optimization of the structural parameters of one of the Schiff's bases in the ground and the excited states were carried out using density functional theory (DFT). The hybrid functional B3LYP was used along with the basis set 6-31G(d). It was assumed that ES IPT

process takes place in synthesized Schiff's bases, as -OH group present adjacent to the =N of imine linkage as well as benzothiazole ring. To focus on the ESIPT process and photophysical properties of Schiff's bases, DFT and TDDFT calculations of one of the Schiff's bases **6a** at the ground and the excited states were carried out using Gaussian software package [58].

3.3.1. Different possible conformers of Schiff's base **6a**:

< **Please insert Figure 5:** Different possible conformers of Schiff's base **6a** in gas phase at ground state >

The Schiff's base **6a** contains the naphthalene core with the benzothiazole ring at 3-position of the naphthalene ring along with the substituted phenylimine linkage at 1-position and -OH group at 2-position. In this type of molecules 16 conformers are possible arising out of single bond rotation. The different conformers and tautomers of the Schiff's base **6a** are illustrated in **Figure 5**. The rotation of the free benzothiazole ring as well as the phenyl ring present on the imine linkage can form different conformers. Also depending upon the direction of -OH group, the different conformers can also exist.

The energy calculations of these conformers and their tautomers in vacuum ground state were carried out (**Table 3**). The computational results show that **6a-Enol 4** has the least energy as compared to the other conformers. **Enol 4** is the predominant species existing among the enol forms in the ground state.

< **Please insert Table 3:** B3LYP/6-31G(d) optimized energy (Kcalmol^{-1}) of enol conformers of Schiff's base **6a** in gas phase at ground state >

Optimization of **Enol 4** form and its tautomer **Keto 4** in vacuum phase as well as in the solvents of different polarities in the ground and the excited state were carried out using the

method B3LYP/6-31G(d). The optimized structures in highly polar aprotic (DMF) and non polar (chloroform) solvents in the ground state are shown in **Figures 6** and **S6**.

< **Please insert Figure 6:** B3LYP/6-31G(d) optimized structure of **6a-Enol** and **6a-Keto** at ground state in DMF >

To impose planarity in the structure, dihedral angle between the naphthalene and the benzothiazole ring as well as that between the phenyl ring on the imine linkage were made to be zero. Due to this, all conformers are in plane initially but changed a little on optimization cycles. The values of the bond lengths and Mulliken charge distributions of **6a-Enol** and its tautomer **6a-Keto** are given in the supporting information (**Tables S6-S9**). Though, it was observed that -OH of the enol is little elongated as compared to the standard O-H bond length in the ground state and is indicative of a strong hydrogen bonding. The hydrogen bonding is also present with a fair bond length of 1.75 Å between N-H in keto structure. The energy computations show that **6a-Keto** form has a lower energy as compared to **6a-Enol** form in vacuum and solvent phases (**Table 4**). Thus **6a-Keto** form exists predominantly in the ground state.

< **Please insert Table 4:** B3LYP/6-31G(d) optimized energy calculations of **6a-Enol** and **6a-Keto** in gas phase and solvent phase at ground state >

3.3.2. Vibrational frequencies:

Also the vibrational frequencies of **6a-Keto** in vacuum at the ground state are matched with that obtained from FT-IR analysis as shown in **Table 5**. There is no broad peak observed at around 3500-3600 cm^{-1} suggests the absence of -OH group and confirms the existence of the keto form.

< **Please insert Table 5:** Observed and calculated vibrational frequencies of **6a-Keto** >

3.3.3. Solvatochromism study:

The structure optimizations studies and energy computations show that the Schiff's base **6a** mainly exists in the keto form. The absorption maxima observed experimentally is much closer to the value obtained from the vertical excitation of the keto tautomer as compared to that of the enol one. The experimental values of the absorption and the vertical excitation of both the enol and the keto forms obtained from TDDFT calculation in different solvents and % deviation values are tabulated in **Table 6**. The % deviation values proved that the experimental absorption wavelength is closer to the computed vertical excitation of **6a-Keto**. The % deviation between the experimental and the computed absorption maxima ranges from 0.8 to 3.7. This observation is in accordance with previous implication that the keto tautomer is predominant in the ground state. In all solvents, the prominent absorption can be assigned to HOMO(H)→LUMO(L) transition (**Table 6**). The FMO 103 is HOMO (H) and FMO 104 is LUMO (L) in all cases.

< **Please insert Table 6:** Experimental UV-visible excitation and computed vertical excitation of **6a** in different solvents from TD-B3LYP/6-31G(d)>

The electronic transitions in the perspective of the molecular orbital picture, the molecular HOMOs and molecular LUMOs were generated by using Gauss View 5.0 software [61]. The HOMO and LUMO graphs of **6a** in the keto form at the ground and the excited states are given in **Table 7**. It has been observed that in the ground state the electron density is localized on the benzothiazole ring as it acts as an acceptor. In the ground and the excited LUMO, the electron density distribution is equal on the entire molecule. Furthermore it transfers to HOMO of the naphthalene core and the imine linkage in the excited state.

< **Please insert Table 7:** Frontier molecular orbital of **6a-keto** in CHCl₃ at ground and excited states.>

3.3.4. Fluorescence emission study:

The experimentally obtained fluorescence emission wavelength and the computed emission wavelength using TD-B3LYP/6-31G(d) and % deviation values are tabulated in **Table 8**. It was observed that the experimental emission is closely related to the computed emission obtained from **6a-Keto***. The emission values computed from the enol form is observed to be larger than the experimental value. The % deviation of **6a-Keto*** from the experimentally observed emission wavelength is lower than **6a-Enol***. The % deviation between the experimental and the theoretical emission wavelengths ranges from 4.2 to 8.9. This contradictory result confirms that the emission of **6a** is due to the keto form and not the enol conformer.

All these computational results confirmed that ESIPT process is not observed in synthesized Schiff's base **6a**.

< **Please insert Table 8:** Experimental emission and computed emission of **6a** in different solvents from TD-B3LYP/6-31G(d)>

4. Conclusion:

In this paper we report the syntheses of a series of Schiff's bases from 3-(1,3-benzothiazol-2-yl)-2-hydroxynaphthalene-1-carbaldehyde by a simple method. Although a -OH group is present ortho to the benzothiazole ring as well as the imine linkage, these dyes do not exhibit ESIPT phenomenon. This was confirmed by DFT computation study of one of the Schiff's bases **6a**. The optimized geometries obtained from B3LYP/6-31G(d) and TD-B3LYP/6-31G(d) were examined by comparing the ground and the excited state geometries and the charge distribution. This study reveals that the keto form is more stable than the enol form in the ground state as against the fact of ESIPT process. The dye **6a** showed a prominent absorption due to HOMO → LUMO transition. The computed absorption and emission wavelengths of the keto

form are in good agreement with the experimental results. The solvatochromism study of all the Schiff's bases proves that the absorbance and fluorescence quantum yield are influenced by the solvent polarity. The TGA analyses reveal that all Schiff's bases are thermally stable.

Acknowledgements:

Manjaree Satam and Rahul Telore are thankful to UGC-CAS for providing research fellowship under Special Assistance Programme (SAP).

References:

1. Tao T, Xu F, Chen XC, Liu QQ, Huang W, You XZ. *Dyes Pigm* 2011; 92:916-922.
2. Vladimirova MP, Simova SD, Stanoeva ER, Mitewa MI. *Dyes Pigm* 2001; 50:157-162.
3. Nelson SM. *Pure Appl Chem* 1980; 52:2461-2476.
4. Vance AL, Alcock NW, Heppert JA, Busch DH. *Inorg Chem* 1998; 37:6912-6920.
5. Johnson CP, Atwood JL, Steed JW, Bauer CB, Rogers RD. *Inorg Chem* 1996; 35:2602-2610.
6. Alizadeh N, Ershad S, Naeimi H, Sharghi H, Shamsipur M. *Pol J Chem* 1999; 73:915-925.
7. Naeimi H, Safari J, Heidarneshad A. *Dyes Pigm* 2007; 73:251-253.
8. Souza P, Garcia-Vazquez JA, Masaguer JR. *Transit Metal* 1985; 10: 410-412.
9. Ispir E. *Dyes Pigm* 2009; 82:13-19.
10. Aksuner N, Henden E, Yilmaz I, Cukurovali A. *Dyes Pigm* 2009; 83:211-217.
11. Oter O, Ertekin K, Kılınçarslan R, Ulusoy M, Cetinkaya B. *Dyes Pigm* 2007; 74:730-735.
12. Ray D, Bharadwaj PK. *Inorg Chem* 2008; 47:2252-2254.
13. Kim HM, Yang PR, Seo MS, Yi JS, Hong JH, Jeon SJ, Ko YG, Lee KJ, Cho BR. *J Org Chem* 2007; 72:2088-2096.

14. Komatsu H, Iwasawa N, Citterio D, Suzuki Y, Kubota T, Tokuno K, Kitamura Y, Oka K, Suzuki K. *J Am Chem Soc* 2004; 126:16353-16360.
15. Suzuki Y, Komatsu H, Ikeda T, Saito N, Araki S, Citterio D, Hisamoto H, Kitamura Y, Kubota T, Nakagawa J, Oka K, Suzuki K. *Anal Chem* 2002; 74:1423-1428.
16. Farruggia G, Iotti S, Prodi L, Montalti M, Zaccheroni N, Savage PB, Trapani V, Sale P, Wolf FI. *J Am Chem Soc* 2006; 128:344-350.
17. Banthia S, Samanta A. *J Phys Chem B* 2006; 110:6437-6440.
18. Que EL, Domaille DW, Chang CJ. *Chem Rev* 2008; 108:1517-1549.
19. Kim HJ, Park SY, Yoon S, Kim JS. *Tetrahedron* 2008; 64:1294-1300.
20. Jung HJ, Singh N, Jang DO. *Tetrahedron Lett* 2008; 49:2960-2964.
21. Hadjoudis E, Mavridis IM. *Chem Soc Rev* 2004; 33:579-588.
22. Forés M, Duran M, Solà M. *Chem Phys* 2000; 260:53-64.
23. Singh N, Kaur N, Mulrooney RC, Callan JF. *Tetrahedron Lett* 2008; 49:6690-6692.
24. Udhayakumari D, Saravanamoorthy S, Ashok M, Velmathi S. *Tetrahedron Lett* 2001; 52:4631-4635.
25. Hazneci C, Ertekin K, Yenigul B, Cetinkaya E. *Dyes Pigm* 2004; 62: 35-41.
26. Hynes JT, Klinman JP, Limbach HH, Schowen RL, Editors. *Hydrogen Transfer Reactions*. Weinheim: Wiley-VCH; 2006.
27. Muller A, Rataiczak H, Junge W. *Electron and Proton Transfer in Chemistry and Biology*. In: Diemann E, Editor. *Studies in Physical and Theoretical Chemistry*. Amsterdam: Elsevier; 1992.
28. Chou P, McMorrow D, Aartsma TJ, Kasha M. *J Phys Chem* 1984; 88:4596-4599.
29. Acuna AU, Costela A, Munoz JM. *J Phys Chem* 1986; 90:2807-2808.

30. Tarkka RM, Zhang X, Jenekhe SA. *J Am Chem Soc* 1996; 118:9438-9439.
31. (a) Wu Y, Peng X, Fan J, Gao S, Tian M, Zhao J, Sun S. *J Org Chem* 2007; 72:62-66. (b) Nagaoka S, Hirota N, Sumitani M, Yoshira K. *J Am Chem Soc* 1983; 105:4220-4226.
32. Sytnik A, Del Valle JC. *J Phys Chem* 1995; 99:13028-13032.
33. Seo J, Kim S, Park SY. *J Am Chem Soc* 2004; 126:11154-11155.
34. Frey W, Elsaesser T. *Chem Phys Lett* 1992; 189:565-570.
35. Kelly R, Schulman S, Schulman S. *Molecular Luminescence Spectroscopy, Methods and Applications Part -2, Chapter 6*. New York: Wiley Interscience; 1988.
36. Cheng YM, Pu SC, Hsu CJ, Lai CH, Pi T. *Chem Phys Chem* 2006; 7(6):1372-1381
37. Guha D, Mandal A, Koll A, Filarowski A, Mukherjee S. *Spectrochim Acta A* 2000; 56:2669-2677.
38. Mandal A, Fitzmaurice D, Waghorne E, Koll A, Filarowski A, Guha D, Mukherjee S. *J Photochem Photobiol A* 2002; 153:67-76.
39. Joshi H, Kamounah FS, Gooijer C, van der Zwan G, Antonov L. *J Photochem Photobiol A* 2002; 152:183-191.
40. Yushchenko DA, Shvadchak VV, Klymchenko AS, Duportail G, Pivovarenko VG, Mély Y. *J Phys Chem A* 2007; 111:10435-10438.
41. Jie H, Aidong P, Hongbing F, Ying M, Tianyou Z, Jiannian Y. *J Phys Chem A* 2006; 110:9079-9083.
42. Barilero T, Le ST, Gosse C, Jullien L. *Anal Chem* 2009; 81:7988-8000.
43. Sheikhshoaie I, Fabian WMF. *Dyes Pigm* 2006; 70:91-98.
44. Satam MA, Telore RD, Tathe AB, Gupta VD, Sekar N. *Spectrochim Acta A* 2014; 127:16-24.

45. Magde D, Wong R, Seybold PG. *Photochem Photobiol* 2002; 75:327-334.
46. Reichardt C, *Solvent and solvent effects in organic chemistry* Third and enlarged edition, Weinheim: Wiley VCH Verlag GmbH & Co. KGaA; 2003.
47. Treutler O, Ahlrichs R. *J Chem Phys* 1995; 102:346-254.
48. Becke AD. *J Chem Phys* 1993; 98:1372-1377.
49. Lee C, Yang W, Parr RG. *Phys Rev B* 1988; 37:785-789.
50. Casida ME, Jamorski C, Salahub DR. *J Chem Phys* 1998; 108:4439-4449.
51. Hehre WJ, Radom L, Schleyer PvR, Pople J. *Ab initio molecular orbital theory*. New York: Wiley; 1986.
52. Bauernschmitt R, Ahlrichs R. *Chem Phys Lett* 1996; 256:454-464.
53. Furche F, Rappaport D. *Density functional theory for excited states: equilibrium structure and electronic spectra*. In: Olivucci M, editor. *Computational Photochemistry*, vol. 16. Amsterdam: Elsevier; 2005 [Chapter 3].
54. Lakowicz, JR. *Principles of Fluorescence Spectroscopy*, 2nd ed. Kluwer, Academic/ Plenum Publishers: New York, 1999.
55. Valeur B. *Molecular fluorescence: principles and applications*. Weinheim: Wiley-VCH Verlag; 2001.
56. Cossi M, Barone V, Cammi R, Tomasi J. *Chem Phys Lett* 1996; 255:327-335.
57. Tomasi J, Mennucci B, Cammi R. *Chem Rev* 2005; 105:2999-3094.
58. Frisch MJ, Trucks GW, Schlegel HB, Scuseria GE, Robb MA, Cheeseman JR *et al.* *Gaussian 09 revision C01*. Wallingford CT: Gaussian Inc; 2010.
59. Anthony K, Brown RG, Hepworth JD, Hodgson KW and May B. *J Chem Soc Perkin Trans II* 1984; 12:2111-2117.

60. Raju BC, Theja ND, Kumar JA. Synth Commun 2009; 39:175-188.

61. Dennington R, Keith T, Millam J. Gauss view version 5.0. Shawnee Mission KS: Semichem Inc; 2009.

ACCEPTED MANUSCRIPT

Scheme 1: Synthetic scheme of Schiff's bases **6a-6f** from 3-(1,3-benzothiazol-2-yl)-2-hydroxynaphthalene-1-carbaldehyde **4**.

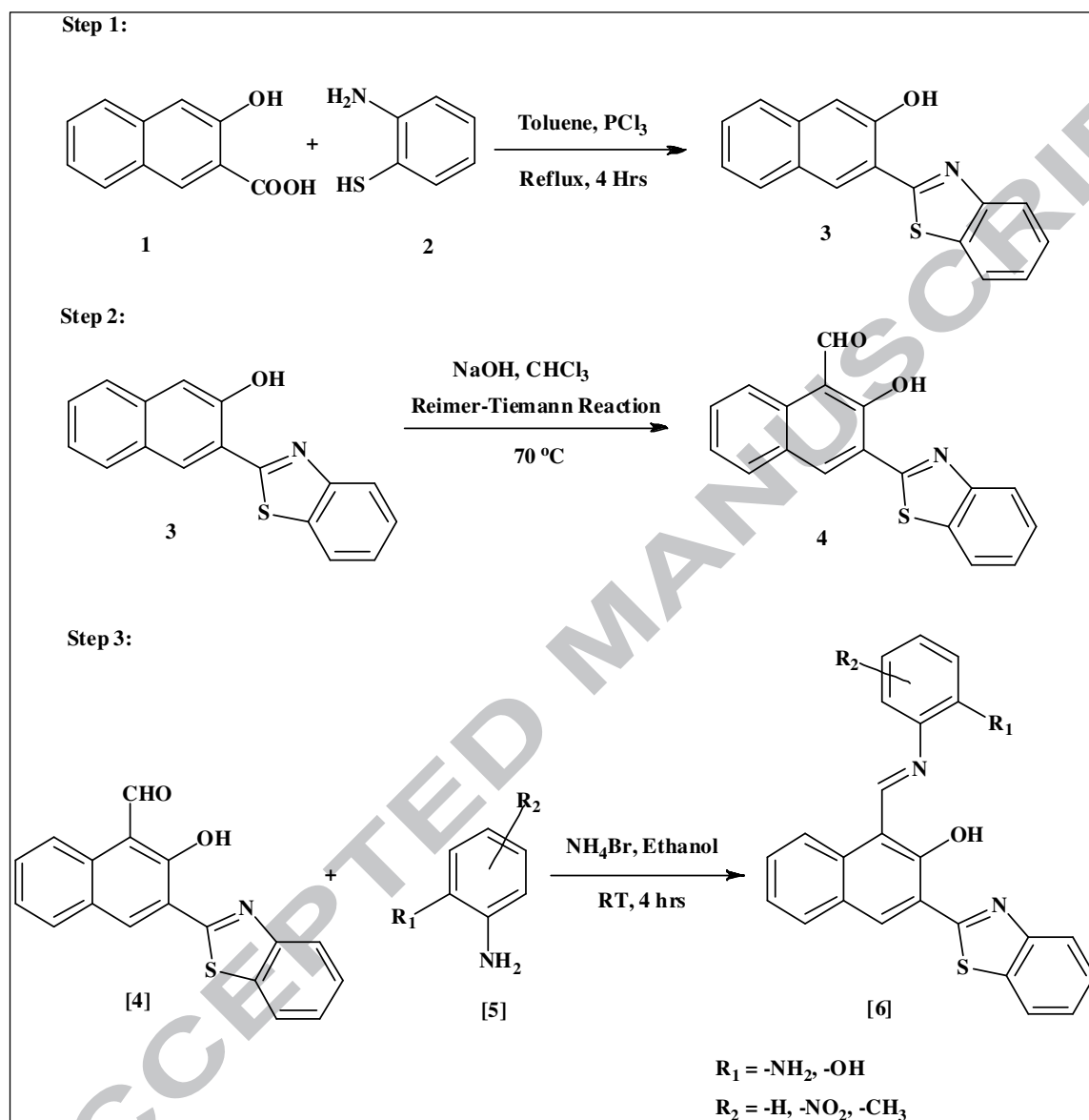
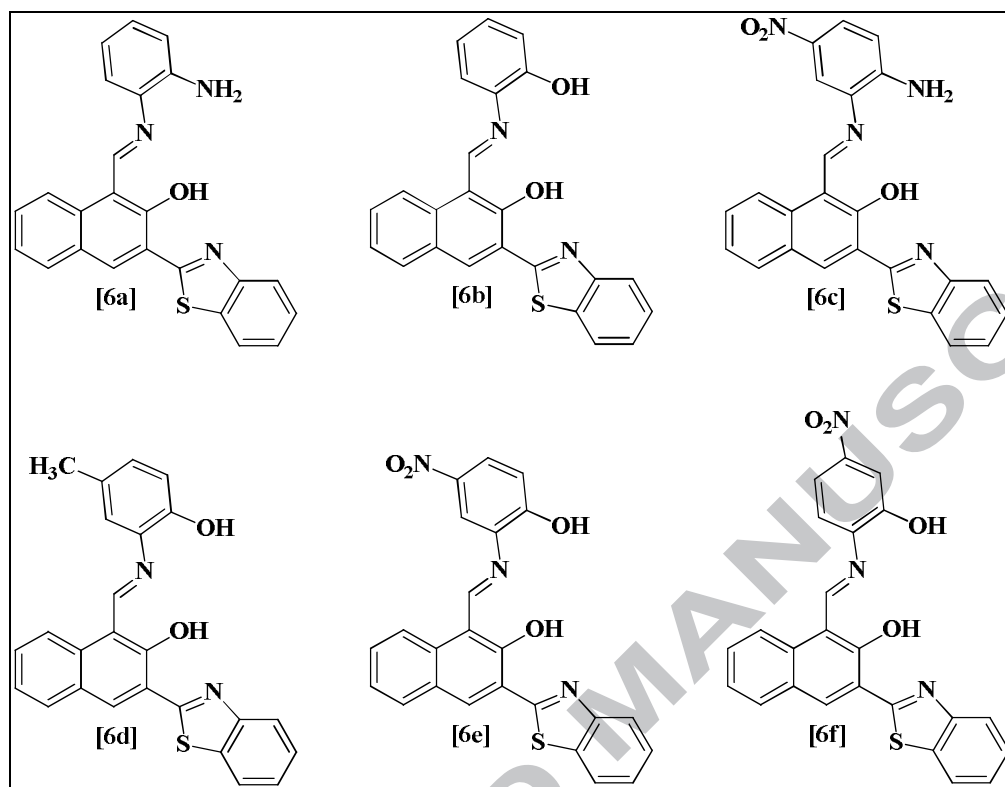


Figure 1: Structures of the synthesized Schiff's bases **6a-6f**.**Figure 2:** ES IPT process observed in known molecules.

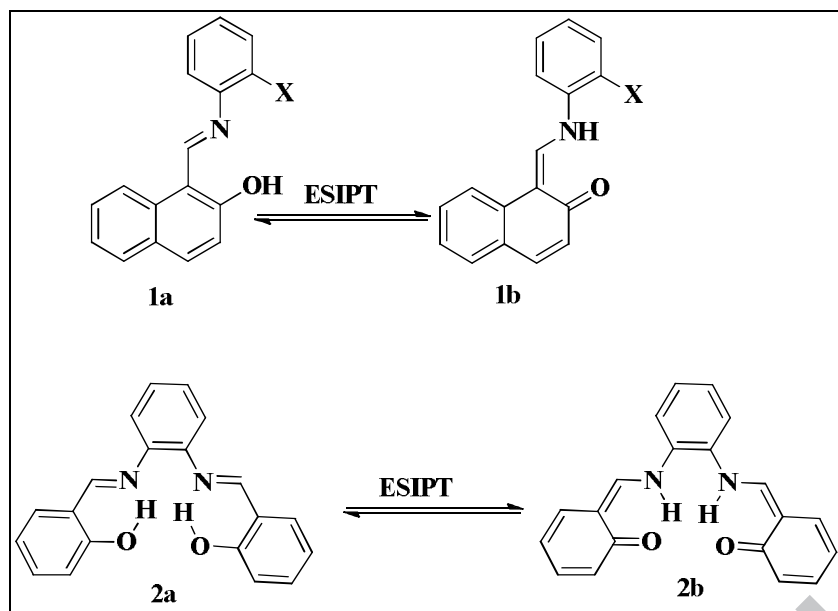
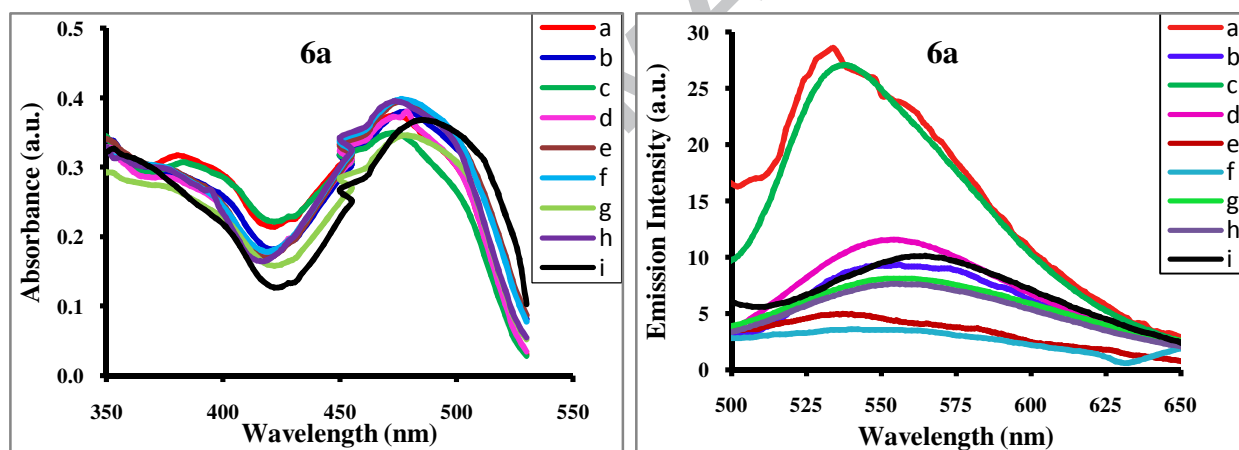


Figure 3: Effect of solvent polarity on photophysical properties of Schiff's base 6a.



Where, a = DCM, b = THF, c = Chloroform, d = Ethyl acetate, e = Acetone, f = Methanol, g = Ethanol, h = Acetonitrile, i = DMF

Figure 4: Thermo gravimetric analysis of Schiff's bases 6a-6f.

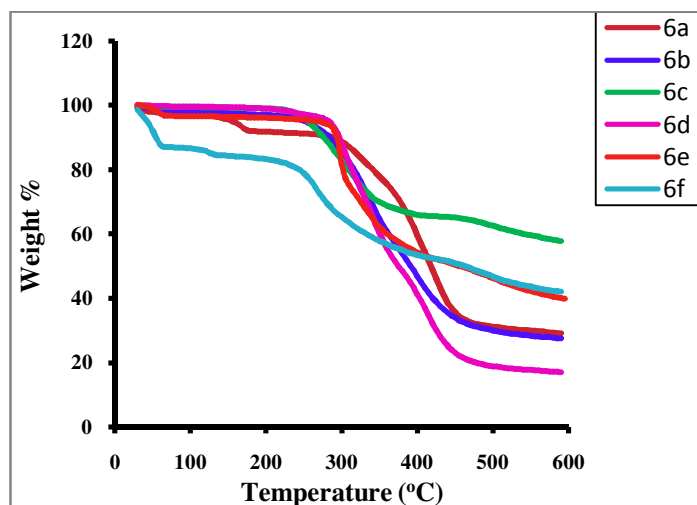


Figure 5: Different possible conformers of Schiff's base **6a** in gas phase at ground state.

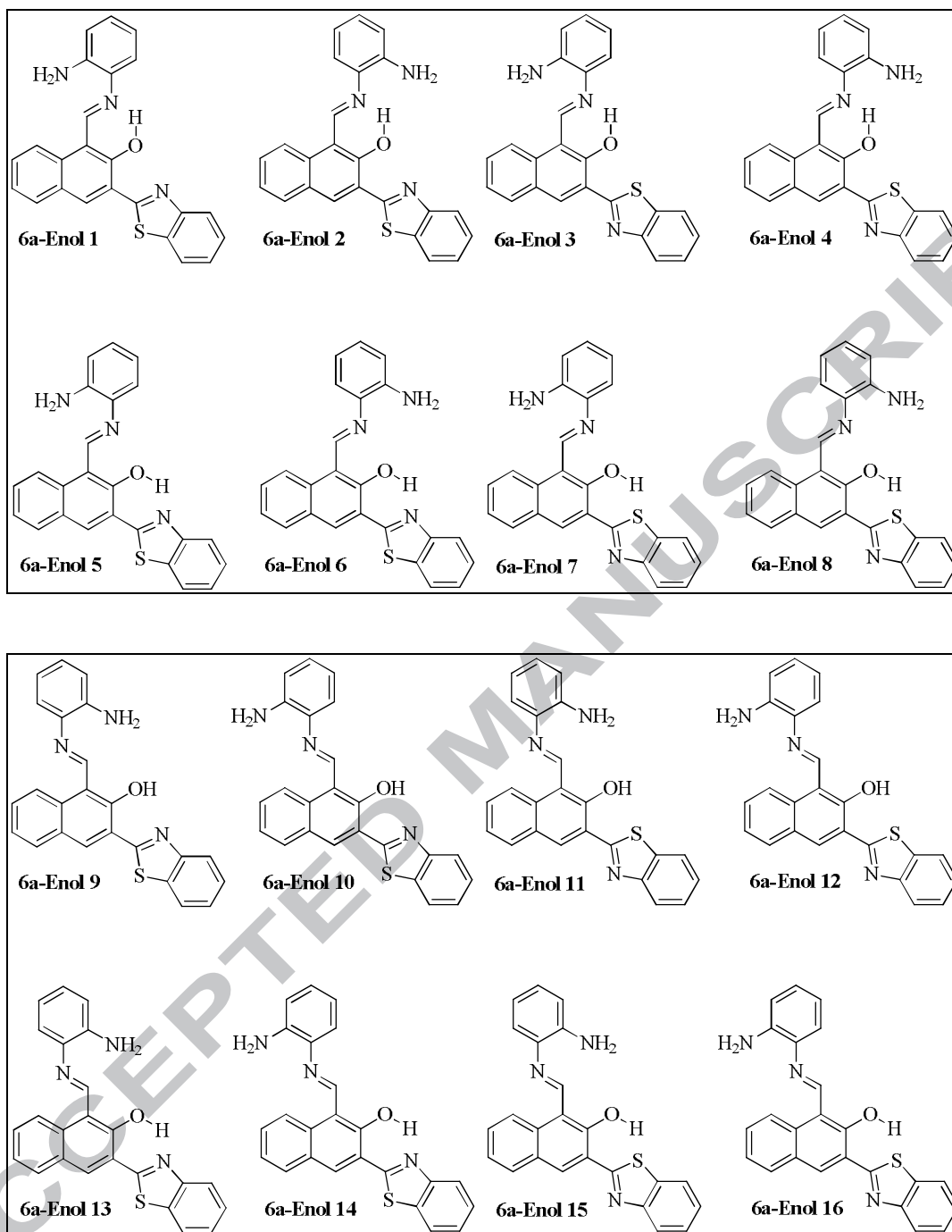
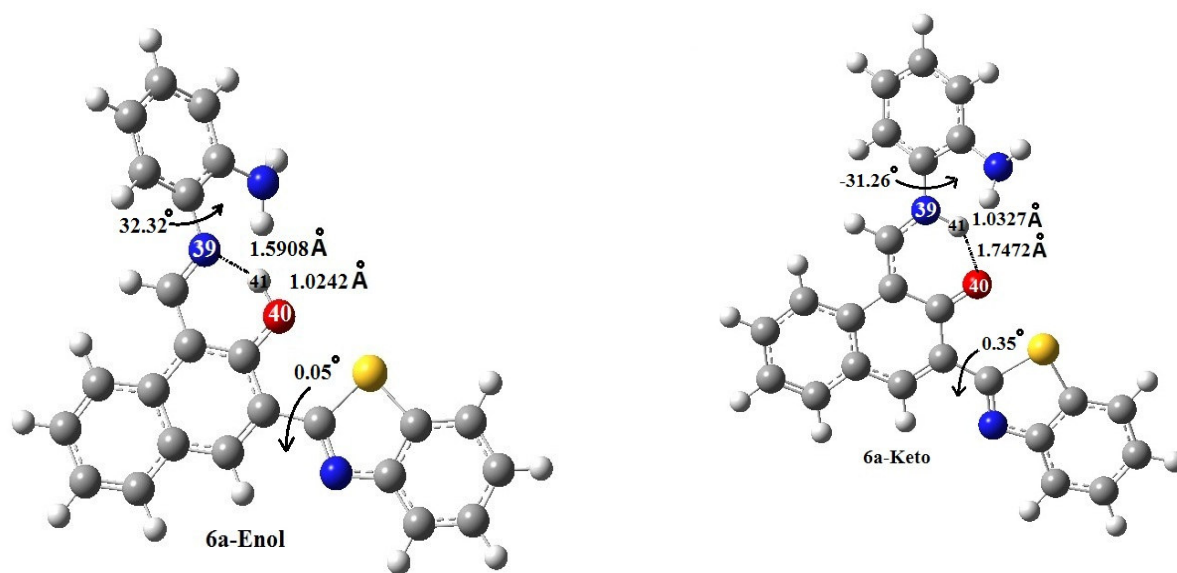


Figure 6: B3LYP/6-31G(d) optimized structure of **6a-Enol** and **6a-Keto** at ground state in DMF.



ACCEPTED MAN

Table 1: Absorption- excitation- emission data of Schiff's base **6a**.

Solvent	λ_{abs}^{max} (nm)	ϵ ($\text{dm}^3\text{mol}^{-1}\text{cm}^{-1}$)	λ_{exc}^{max} (nm)	λ_{ems}^{max} (nm)	$\Delta\lambda$ (nm)	$\Delta\lambda$ (cm^{-1})	Φ
DCM	470	15168	490	534	64	2550.0	0.029
THF	479	15563	486	556	77	2891.2	0.012
Chloroform	467	13548	498	540	73	2894.7	0.013
Ethyl acetate	473	14733	484	554	81	3091.1	0.080
Acetone	473	15484	484	545	72	2793.0	0.012
Methanol	476	15721	482	554	78	2957.8	0.007
Ethanol	476	13627	492	554	78	2957.8	0.004
Acetonitrile	476	15563	498	556	80	3022.7	0.017
DMF	482	14457	494	565	83	3047.7	0.024

Table 2: Thermo gravimetric analysis of Schiff's bases **6a-6f**.

Compound	TGA ($^{\circ}\text{C}$)	Compound	TGA ($^{\circ}\text{C}$)
6a	280 (90.51%)	6d	285 (94.55%)
6b	270 (92.65%)	6e	270 (94.88%)
6c	250 (95.98%)	6f	235 (81.06%)

Table 3: B3LYP/6-31G(d) optimized energy (Kcalmol⁻¹) of enol conformers of Schiff's base **6a** in gas phase at ground state.

Conformer	Energy	Conformer	Energy
6a-Enol 1	-980472.5	6a-Enol 9	-980459.9
6a-Enol 2	-980475.5	6a-Enol 10	-980463.9
6a-Enol 3	-980477.5	6a-Enol 11	-980463.6
6a-Enol 4	<u>-980480.3</u>	6a-Enol 12	-980467.5
6a-Enol 5	-980473.8	6a-Enol 13	-980473.7
6a-Enol 6	-980473.8	6a-Enol 14	-980477.7
6a-Enol 7	-980464.6	6a-Enol 15	-980463.7
6a-Enol 8	-980464.6	6a-Enol 16	-980467.7

Table 4: B3LYP/6-31G(d) optimized energy calculations of **6a-Enol** and **6a-Keto** in gas phase and solvent phase at ground state.

Phase/ Solvent	Energy of 6a-Enol (Kcal mol ⁻¹)	Energy of 6a-Keto (Kcal mol ⁻¹)
Gas	-980480.3	-980483.1
DCM	-980491.7	-980496.5
Chloroform	-980489.6	-980494.0
Ethyl acetate	-980486.3	-980490.4

Acetone	-980493.3	-980498.4
Acetonitrile	-980494.1	-980499.3
DMF	-980488.2	-980492.8

Table 5: Observed and calculated vibrational frequencies of **6a-Keto**.

Bond	Vibrational frequency (observed) cm⁻¹	Vibrational frequency (calculated) cm⁻¹
-C=O (keto)	1608	1608
-C=N (benzothiazole)	1545	1539
Aromatic ring	1493	1493
-C=N (imine)	1432	1442
-C-S (benzothiazole)	722	718

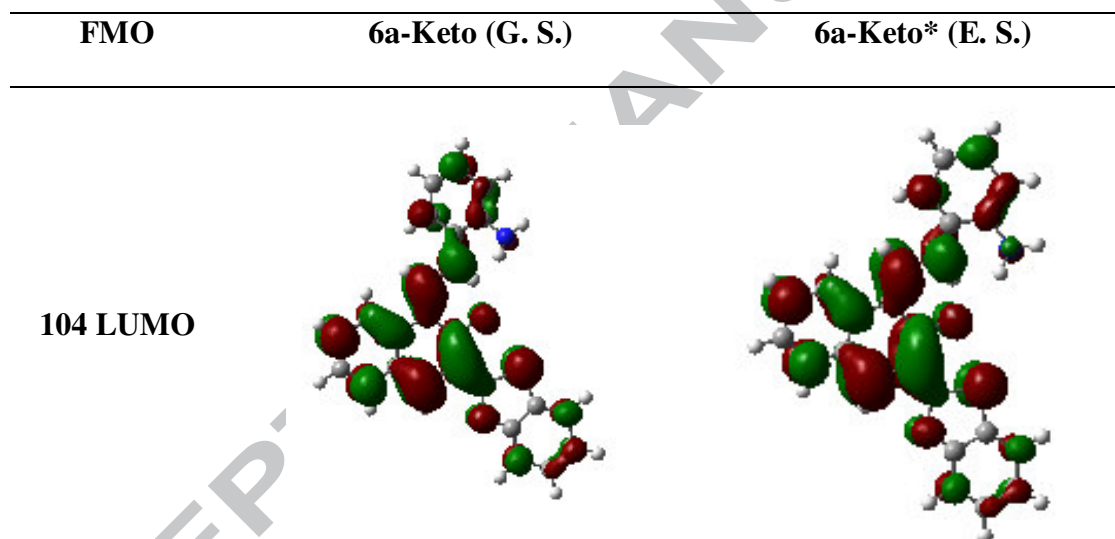
Table 6: Experimental UV-visible excitation and computed vertical excitation of **6a** in different solvents from TD-B3LYP/6-31G(d).

Solvent	$\lambda_{\text{abs}}^{[a]}$	TD-B3LYP/6-31G(d)			Orbital contribution (Keto)	%D^[e]	
		$\lambda_{\text{Enol}}^{[b]}$	$\lambda_{\text{Keto}}^{[c]}$	$(f)^{[d]}$		6a-Enol	6a-Keto
DCM	470	457	465	0.4549	H→L (0.6607)	2.7	1.0
Chloroform	467	456	463	0.4707	H→L (0.6599)	2.3	0.8
Ethyl acetate	473	452	460	0.4644	H→L (0.6999)	4.4	2.7

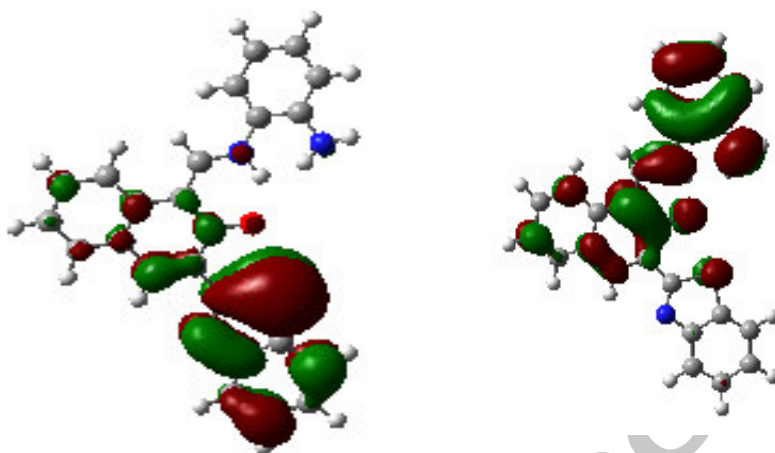
Acetone	473	456	466	0.4363	H→L (0.6604)	3.5	1.4
Acetonitrile	476	457	467	0.431	H→L (0.6605)	3.9	1.8
DMF	482	453	464	0.467	H→L (0.6999)	6.0	3.7

^[a] Experimentally observed absorption wavelength (nm). ^[b] Vertical excitation wavelength (nm) of Enol obtained by DFT computation. ^[c] Vertical excitation wavelength (nm) of Keto obtained by DFT computation. ^[d] Only major contributions are presented; f = oscillator strength. ^[e] %D= % deviation between experimental absorption and computed (TD-DFT) absorption.

Table 7: Frontier molecular orbital of **6a-keto** in CHCl₃ at ground and excited states.



103 HOMO



ACCEPTED MANUSCRIPT

Table 8: Experimental emission and computed emission of **6a** in different solvents from TD-B3LYP/6-31G(d).

Solvent	$\lambda_{\text{emi}}^{[a]}$ (nm)	Computed emission wavelength (nm)		%D ^[b]	
		6a-Enol*	6a-Keto*	6a-Enol*	6a-Keto*
DCM	534	611	582	14.4	8.9
Chloroform	540	611	576	13.1	6.6
Ethyl acetate	554	610	579	10.1	4.5
Acetone	545	613	587	12.4	7.8
Acetonitrile	556	614	589	10.4	5.9
DMF	565	614	589	8.6	4.2

^[a] Experimentally observed emission wavelength (nm). ^[b] %D= % deviation between experimental emission and computed (TD-DFT) emission.

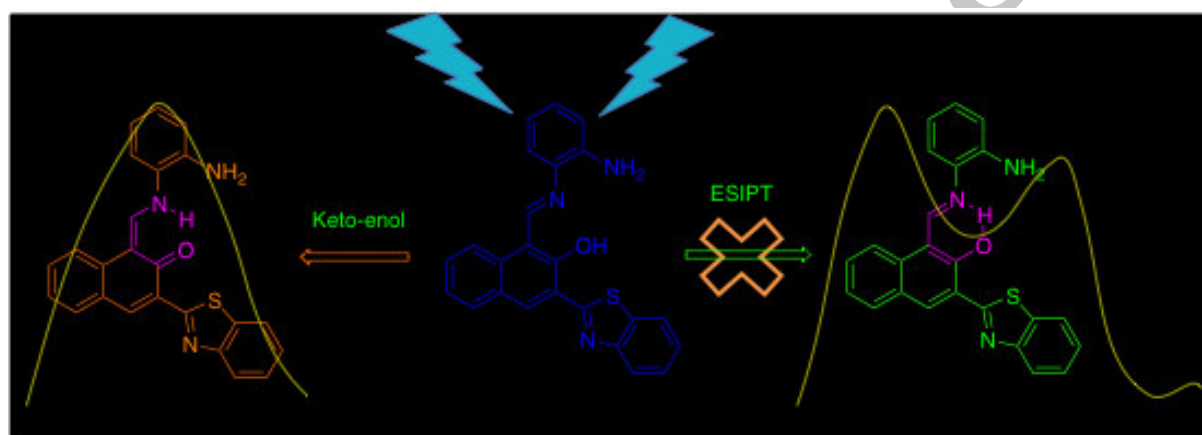
Synthesis and characterization of Schiff's bases from 3-(1,3-benzothiazol-2-yl)-2-hydroxy
naphthalene-1-carbaldehyde

Manjaree A. Satam, Rahul D. Telore, Nagaiyan Sekar*

Tinctorial Chemistry Group, Department of Dyestuff Technology, Institute of Chemical
Technology, Matunga, Mumbai-400 019, India.

E-mail: n.sekar@ictmumbai.edu.in, nethi.sekar@gmail.com

Tel: +91 22 3361 2707; Fax: +91 22 3361 1020.



Presence of hydroxyl group at ortho position to benzothiazole ring as well as imine linkage may lead to the existence of ESIPT process. But computational study of one of the Schiff's bases reveals that keto form is more stable than enol form at ground state in gas as well as in solvent phase. Thus ESIPT process does not exist in synthesized Schiff's bases.

Highlights

- Schiff's bases have been synthesized from ESIPT molecule, 3-(1,3-Benzothiazol-2-yl)-2-hydroxynaphthalene-1-carbaldehyde.
- Photophysical properties of all Schiff's bases have been studied experimentally in different solvents.
- Electronic structure, geometry and photophysical properties of one of the Schiff's bases have been investigated theoretically and correlated to the experimental results.

ACCEPTED MANUSCRIPT